pp 1865–1878. © The Author(s), 2020. Published by Cambridge University Press on behalf of Royal Aeronautical Society
doi:10.1017/aer.2020.65

Ferrofluid thin films for aerofoil lift enhancement and delaying flow separation

F.J. Arias
francisco.javier.arias@upc.edu
Department of Fluid Mechanics
Polytechnic University of Catalonia
ESEIAAT C/Colom 11, 08222 Barcelona
Spain

ABSTRACT

In this work, consideration is given to a novel concept for aerofoil lift enhancement and delaying flow separation. Here, lift enhancement is attained by preventing the growth of the boundary layer through the elimination of the zero-slip condition between the wing surface and the air stream. The concept would simulate all the effects of a moving wall, leading to the appearance of a slip velocity at the gas–fluid interface, including the injection of momentum into the air boundary layer, but with one exception: here there is no moving wall but instead a ferrofluid thin film pumped parallel and attached to the wall by a magnetic field. Utilising a simplified physical model for the velocity profile of the ferrofluid film and based on ferrohydrodynamic stability considerations, an analytical expression for the interfacial velocity is derived. Finally, from the available experimental data on moving walls, the expected lift and angle-of-attack enhancement are found as well as the weight penalty per unit surface area of the wing is estimated. Additional research and development is required to explore the possibilities of using ferrofluid thin films.

Keywords: Flow separation; Boundary layer; Lift enhancement; Aerodynamics

NOMENCLATURE

g	gravity
H	magnetic field
l	thickness of the permanent magnet or ferrofluid
M	magnetisation
p	pressure
Q	volumetric flow
S	surface area of the wing

Received 24 March 2020; revised 27 May 2020; accepted 1 July 2020.

T temperature
u velocity of air
v velocity of ferrofluid
W weight
x length coordinate
z normal coordinate

Greek symbol

δ thickness of the ferrofluid film
η dynamic viscosity
μ magnetic momentum
ρ density
σ surface tension

Subscripts

a air
f ferrofluid
i air–ferrofluid interface
m magnet
o interface

1.0 INTRODUCTION

Almost immediately after Prandtl's boundary-layer theory was proposed, continuous research began to identify methods to mitigate its negative effects. Although a multitude of approaches have been suggested to tackle this problem, all of them in one way or another try to prevent, or at least delay, the detachment of the boundary layer from the wall (e.g. Refs. [1–10]). Suction and blowing, turbulence promoters, vortex generators, and moving walls are just some examples of the various techniques that can be found in literature. The aim of suction and blowing is to remove low-energy air, through suction slots or by blowing high-energy air through backward-directed slots, respectively. On the other hand, turbulence promoters and vortex generators attempt to control the flow separation on symmetric aerofoils by creating spots of high turbulence by using various elements such as baffles or wall roughness elements. Finally, one has moving solid walls, which are intended to remove the zero-slip condition as well as to inject momentum into the boundary layer.

The object of this work is to analyse a novel approach for lift enhancement. According to this concept, this goal is attained by preventing the growth of the air boundary layer through eliminating the zero-slip condition between the surface and the air stream, and more exactly by elimination of the air–wing direct contact. The concept would simulate all effects of a moving wall, leading to the appearance of a slip velocity at the gas–fluid interface, including the injection of momentum into the boundary layer, with one exception: there is no moving wall but instead a ferrofluid thin film pumped parallel and attached to the wall by a magnetic field. For this work, it suffices to know that a ferrofluid or ferromagnetic fluid is nothing more

https://doi.org/10.1017/aer.2020.65 Published online by Cambridge University Press

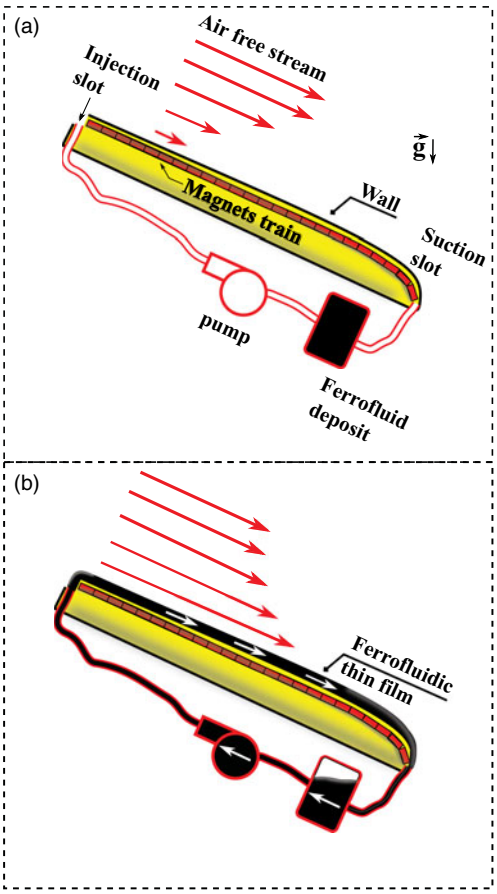

Figure 1. Sketch of the core idea. (a): in normal conditions, the zero-slip condition leads to the formation of a boundary layer, limiting the lift. (b): because of the injection of a ferrofluid thin film attached to the wall by a magnetic field, the zero-slip condition disappears, which translates into lift enhancement.

than a colloidal liquid that becomes strongly magnetised in the presence of a magnetic field due to the presence of suspended nanoscale ferromagnetic, or ferrimagnetic particles. For the sake of illustration, Fig. 1 shows a schematic of the concept investigated in this work. However, caution is called, Fig. 1 is not intended to give a definitive design, nor should it be misconstrued as an attempt to produce a definitive optimised application of the concept, as real applications could depart largely from this sketch. Nonetheless, it provides important guidance on the core idea proposed in this work.

2.0 MATERIALS AND METHODS

2.1 The ferromagnetic thin film layer

To begin, consider Fig. 2, in which a ferrofluid thin film (with a thickness of a few millimetres or less) is attached to the wall of an aerofoil by a magnetic gradient field normal to the

https://doi.org/10.1017/aer.2020.65 Published online by Cambridge University Press

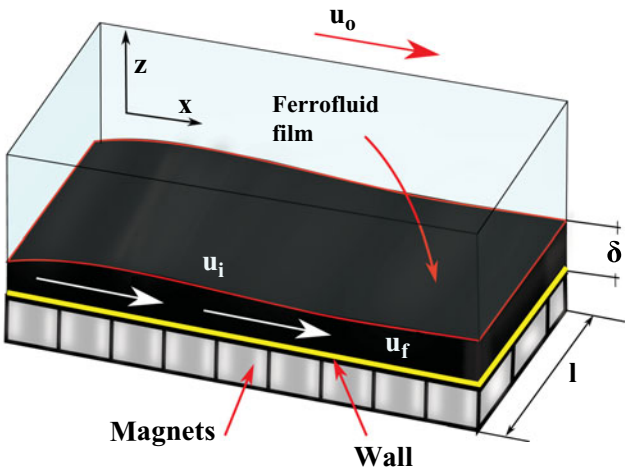

Figure 2. Physical model of the region of the aerofoil covered by the ferrofluid film.

surface which is generated by, say, an array of permanent magnets attached below the wing. In addition, the ferrofluid is pumped tangentially to the surface of the wall. We choose the normal to the surface as the z-axis and the x-axis in the direction of motion of the fluid and fixing the origin of coordinates at the wall. Considering that the velocity depends only on the normal axis z, and that the considered film is a few millimetres thick or less, the convective term in the Navier–Stokes equations can be neglected in comparison with the viscous term, leading to [11]

$$\frac{1}{\eta_f}\frac{\partial p}{\partial x} = \frac{\partial^2 v_x}{\partial z^2}, \qquad \ldots (1)$$

and

$$\frac{\partial p}{\partial z} = \rho_f g + \mu_f M_f \frac{\partial H}{\partial z}, \qquad \ldots (2)$$

where p is pressure; v_x is the ferrofluid velocity parallel to the wall; η_f, ρ_f, M_f, and μ_f are the dynamic viscosity, density, magnetisation, and magnetic momentum of the ferrofluid, respectively; g is gravity; $\frac{\partial H}{\partial z}$ is the uniform normal magnetic gradient. After integrating Equation (2) one obtains

$$p = p_1(x) + \rho_f g z + \mu_f M_f \frac{\partial H}{\partial z} z \qquad \ldots (3)$$

Now, we define the boundary conditions for Equation (1). First, on the solid boundary, the ferrofluid velocity vanishes, which give the first boundary condition as

$$v_x(z = 0) = 0 \qquad \ldots (4)$$

https://doi.org/10.1017/aer.2020.65 Published online by Cambridge University Press

Second, at the air–ferrofluid interface ($z = \delta$), the components of the viscous stress tensor are continuous[12], thus

$$\eta_f \frac{\partial v_x}{\partial z}\bigg|_{z=\delta} + \eta_a \frac{\partial u_x}{\partial z}\bigg|_{z=\delta} = 0, \quad \ldots (5)$$

where u and η_a are the air velocity and dynamic viscosity, respectively. For a very thin film ($\delta \to 0$) and considering that $\eta_f \gg \eta_a$, one can assume that $\eta_f \frac{\partial v_x}{\partial z} \gg \eta_a \frac{\partial u_x}{\partial z}$, in which case Equation (5) simplifies to

$$\eta_f \frac{\partial v_x}{\partial z} \approx 0 \quad \ldots (6)$$

Finally, the discharge or volumetric flow is given by

$$Q = l \int_0^{\delta} v_x(z) \mathrm{d}z \quad \ldots (7)$$

Taking into account the set of boundary conditions, the solution of Equation (1) yields

$$v_x = \frac{3Q}{2l\delta^2}\left[2z - \frac{z^2}{\delta}\right] \quad \ldots (8)$$

The above equation is familiar from Couette flow with a pressure gradient, as expected[13]. On the other hand, the interfacial velocity $v_x(z = \delta) = v_i$ is

$$v_i = \frac{3Q}{2l\delta}, \quad \ldots (9)$$

and likewise the mean velocity $\bar{v}_x$ is

$$\bar{v}_x = \frac{Q}{\delta l}, \quad \ldots (10)$$

which considering Equation (9) becomes

$$\bar{v}_x = \frac{2v_i}{3} \quad \ldots (11)$$

2.2 Film stability

From Equation (8), one may be tempted to think that, by increasing the volumetric flow indefinitely, i.e. the pumping power, or by decreasing the thickness of the film, it could be possible to increase the interface velocity as desired. However, this is not the case. Actually, the maximum interface velocity is limited by Kelvin–Helmholtz instabilities which arise from the relative motion between the ferrofluid and the air stream. The criterion for instability in the magnetic Kelvin–Helmholtz problem when the ferrofluid film is under the action of a magnetic field is given by,[11]

$$(\bar{v}_x - u_o)^2 > \frac{\rho_f + \rho_a}{\rho_f \rho_a}\left[2\left[g(\rho_f - \rho_a)\sigma\right]^{\frac{1}{2}} + \frac{(\mu_a - \mu_f)^2 H_x^2}{\mu_a + \mu_f}\right], \quad \ldots (12)$$

https://doi.org/10.1017/aer.2020.65 Published online by Cambridge University Press

where $\bar{v}_x$ is the mean ferrofluid velocity, u_o is the air free stream velocity; ρ_f and ρ_a are the density of the ferrofluid and the air, respectively; g is gravity; σ is the surface tension, μ_a and μ_f are the magnetic permeability of the air and the ferrofluid, respectively. In the above equation, the uniform magnetic field H_x is the magnetic field collinear with the direction of wave propagation (the stream direction), where it is known that a tangential applied magnetic field in the direction normal to the direction of wave propagation offers no stabilisation[11].

Because $\rho_a \ll \rho_f$ and $\mu_a \ll \mu_f$, and taking into account Equations (11) and (12) becomes

$$\frac{v_i}{u_o} > \frac{3}{2}\left[1 + \frac{1}{u_o}\left[\frac{2(g\rho_f\sigma)^{\frac{1}{2}} + \mu_f H_x^2}{\rho_a}\right]^{\frac{1}{2}}\right] \quad \ldots(13)$$

However, although a uniform magnetic field normal to the direction of wave propagation provides null stabilisation, a magnetic gradient in this direction causes a normal body force per unit volume of

$$F_m = \mu_0 M_f \nabla_z H, \quad \ldots(14)$$

where μ_0 is the permeability of free space, M_f is the magnetisation of the ferrofluid and $\nabla_z H$ is the normal magnetic field gradient. Thus, because both gravity and the magnetic force are body forces, an effective acceleration g_e may be defined as

$$g_e = g + \frac{\mu_0 M \nabla_z H}{\rho_f} \quad \ldots(15)$$

Therefore, if only a gradient magnetic field is acting on the ferrofluid plus gravity and surface tension, the stability criterion in Equation (13) becomes

$$\frac{v_i}{u_o} > \frac{3}{2}\left[1 + \frac{1}{u_o}\left[\frac{2\sigma^{\frac{1}{2}}(g\rho_f + \mu_0 M_f \nabla_z H)^{\frac{1}{2}}}{\rho_a}\right]^{\frac{1}{2}}\right] \quad \ldots(16)$$

3.0 DISCUSSION

To obtain some idea of the shape of the curves predicted by Equations (13) and (16), we assume some typical values of the parameters for a ferrofluid: $\sigma = 70 \times 10^{-3}$N/m; $g = 9.8$m/s^2; $\rho_f = 1.2 \times 10^3$kg/m^3; $\rho_a = 1.0$kg/m^3; $M_f = 4.5 \times 10^5$A/m, which corresponds to a realisable magnetic field of around 0.5T obtained from a typical hand-held permanent magnet; $\mu_0 = 4\pi \times 10^{-7}$H/m; $\mu_f = 8\mu_0$. The resulting curves are shown in Figs. 3 and 4 for Equations (13) and (16), respectively, and considering practical achievable values for the magnetic field as well as the magnetic gradient.

3.1 Experimental measurements

To obtain a preliminary idea of the lift enhancement when using ferrofluid thin films, full experiments on specific aerofoil designs are not required. Instead, because from an

https://doi.org/10.1017/aer.2020.65 Published online by Cambridge University Press

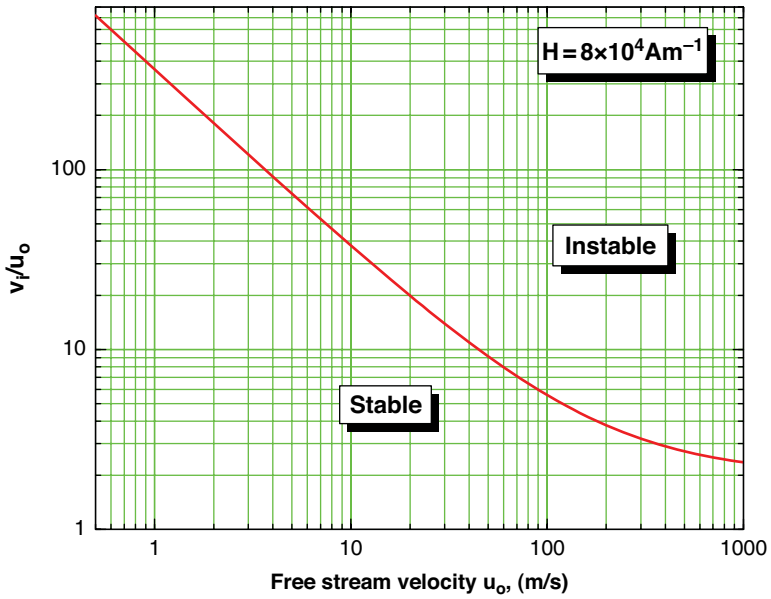

Figure 3. Stability curve predicted by Equation (13) as a function of the air free stream.

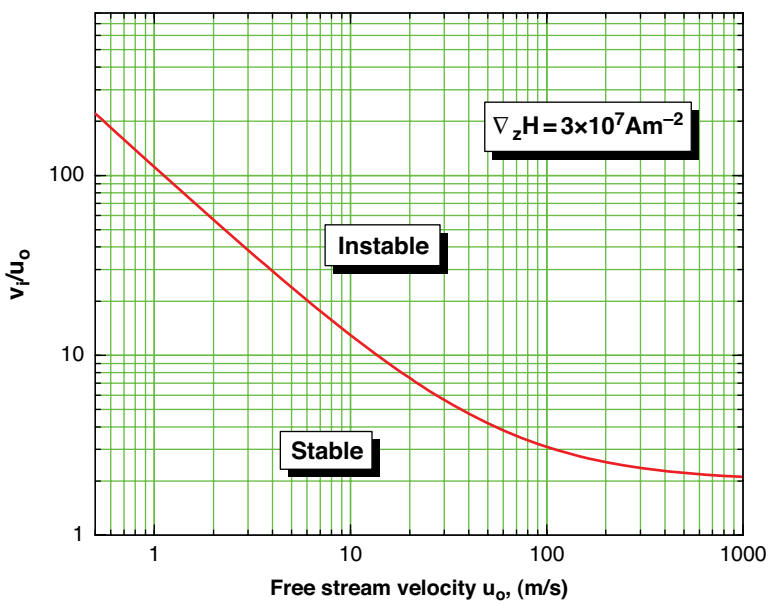

Figure 4. Stability curve predicted by Equation (16) as a function of the air free stream.

aerodynamic point of view there is no substantial difference if the interfacial velocity is generated by a thin film or, say, a moving solid surface, the thin film can be regarded to some extent as a moving solid surface (both being introduced into the differential Navier–Stokes equations as a simple boundary condition), thus it is possible to take advantage of experimental

https://doi.org/10.1017/aer.2020.65 Published online by Cambridge University Press

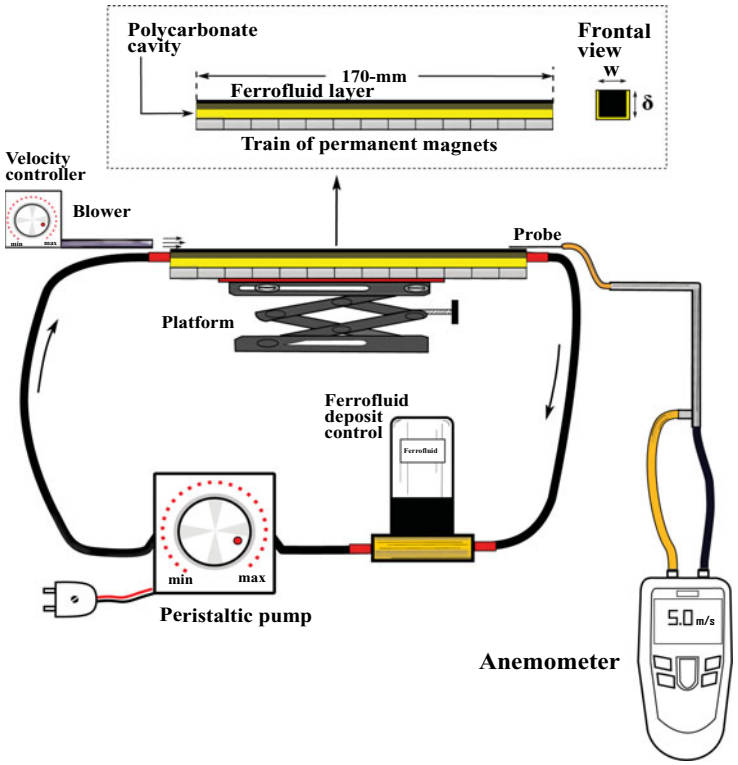

Figure 5. Sketch of the experimental set-up.

measurements available in literature on the lift enhancement and flow separation from moving solid surfaces for several aerofoil designs. Hence, after obtaining experimental measurements of the interfacial velocity from the ferrofluid film, the lift and angle-of-attack can be inferred from the available literature on moving surfaces with the same interfacial velocity. With this goal, a set of experiments were performed to find the attainable interfacial velocity for the concept of the ferrofluid film.

The set-up consisted in a square polycarbonate cavity with $\delta = l$ and 170mm long, filled with ferrofluid. Below the cavity, a train of hand-held neodymium permanent magnets were located. The ferrofluid was pumped through the cavity by using a peristaltic pump, electronically regulated by the number of revolutions per minute. Several cavities were used, i.e. different δ values, but always keeping the same length. The ferrofluid employed was $Mn_{0.5}Zn0.5Fe_2O_4$ in water at room temperature $T = 298$K. The air stream was propelled by a blower parallel to the cavity. The interfacial velocity v_i was measured by using a Fluke 922 airflow meter. The cavity was positioned on a simple laboratory adjustable lifting-rotating platform to allow measurements at different angles of inclination. The magnetic field from the array of magnets was measured as 0.12T at 3mm from its surface using a FW BELL 5170 Gauss/Tesla meter. Figures 5 and 6 show a sketch and the real experimental set-up, respectively.

https://doi.org/10.1017/aer.2020.65 Published online by Cambridge University Press

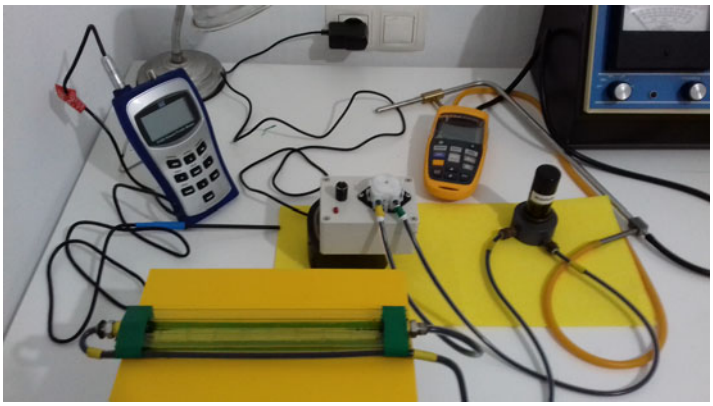

Figure 6. Close-up of experimental set-up.

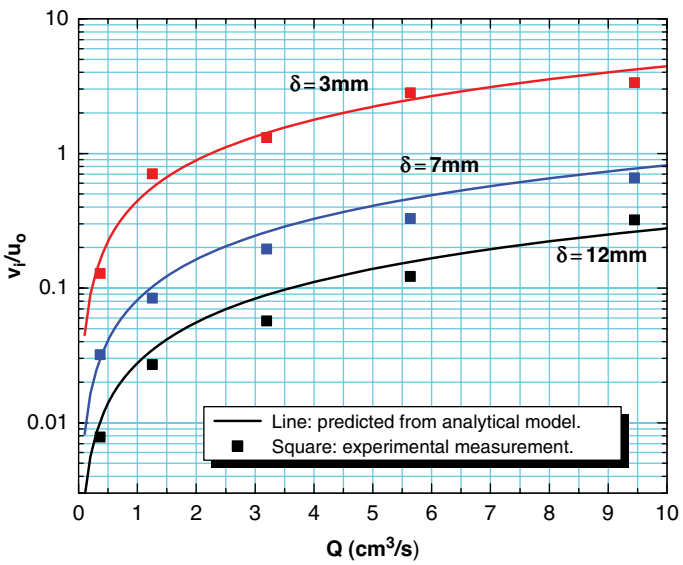

Figure 7. $\frac{v_i}{u_o}$ as a function of the volumetric flow with $u_o = 0.5$m/s.

4.0 RESULTS AND CONCLUSIONS

The resulting experimental curves are shown in Figs. 7, 8, and 9. Figure 7 shows the ratio $\frac{v_i}{u_o}$ as a function of the volumetric flow and for several thicknesses of the cavity. Figure 8 shows the ratio $\frac{v_i}{u_o}$ as a function of the free stream air, and Fig. 9 shows the effect of the angle of inclination (by taking measurements at different inclination angles of the platform from totally horizontal at 0° to totally vertical 90°; see Fig. 5) of the cavity on the ratio $\frac{v_i}{u_o}$ and for several thicknesses of the cavity.

Finally, Figs. 10 and 11 show shows the predicted lift enhancement and the increase of the angle-of-attack for a NACA0015 derived from using the experimental interfacial velocity

https://doi.org/10.1017/aer.2020.65 Published online by Cambridge University Press

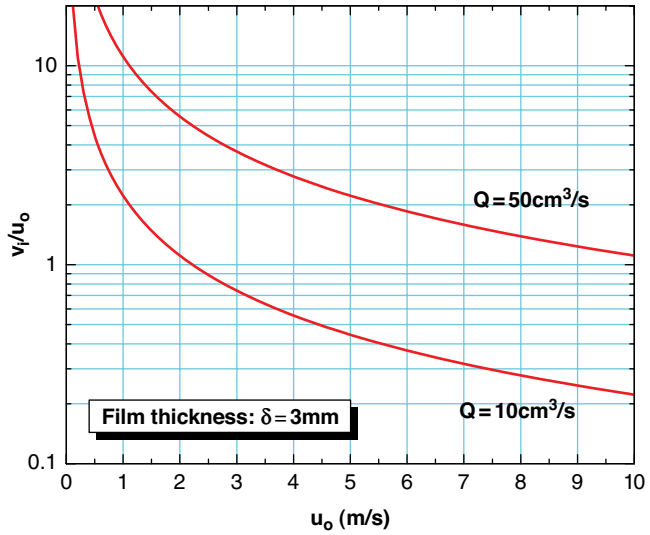

Figure 8. $\frac{v_i}{u_o}$ as a function of the free stream air.

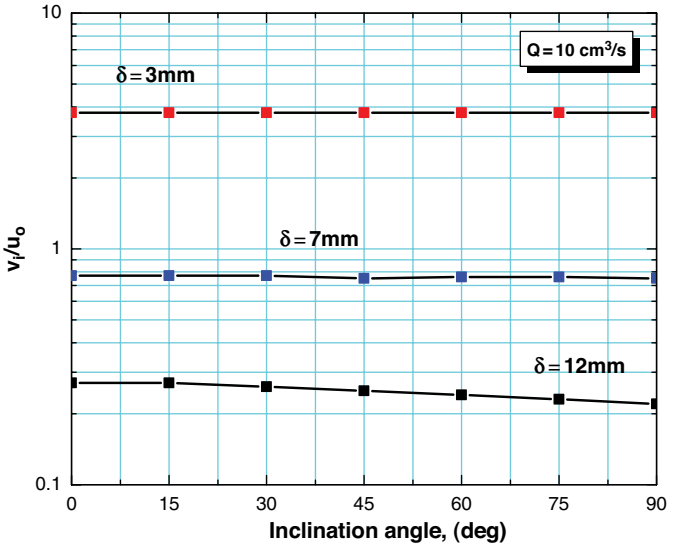

Figure 9. $\frac{v_i}{u_o}$ as a function of the angle of inclination and for several thicknesses of the cavity.

obtained before and applied to the plots of the experimental data on moving walls reported by Ref. [14], i.e. by replacing the velocity of the wall by the interfacial velocity of the film.

It is easy to see the attractiveness of the proposed concept by comparing the lift coefficient enhancement as a function of $\frac{v_i}{u_o}$ in Fig. 10, and the allowable $\frac{v_i}{u_o}$ as a function of the air stream velocity from the curves of ferrohydrodynamic stability in Figs. 3 and 4. Thus, as an

https://doi.org/10.1017/aer.2020.65 Published online by Cambridge University Press

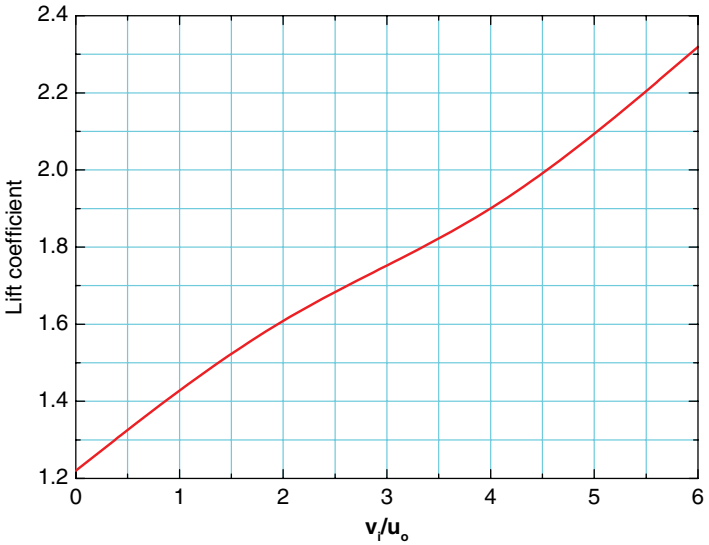

Figure 10. Lift coefficient as a function of $\frac{v_i}{u_o}$.

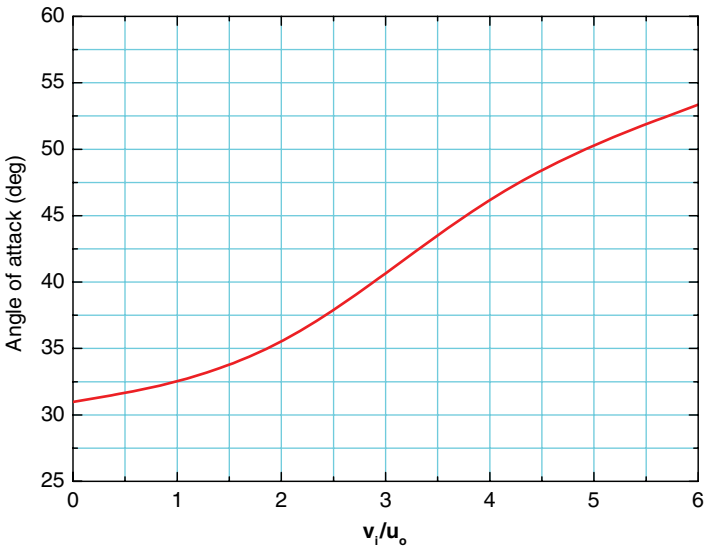

Figure 11. Angle-of-attack as a function of $\frac{v_i}{u_o}$.

illustrative example, an air stream velocity of around 100m/s will allow for a thin film $\frac{v_i}{u_o}$ ratio of around $\approx$ 3m/s before the Kelvin–Helmholtz effect will detach the film. With this ratio, the lift coefficient enhancement could be around 1.8, which is a considerable figure of merit. Additional research and development is required to explore the possibilities of using such ferrofluid thin films.

https://doi.org/10.1017/aer.2020.65 Published online by Cambridge University Press

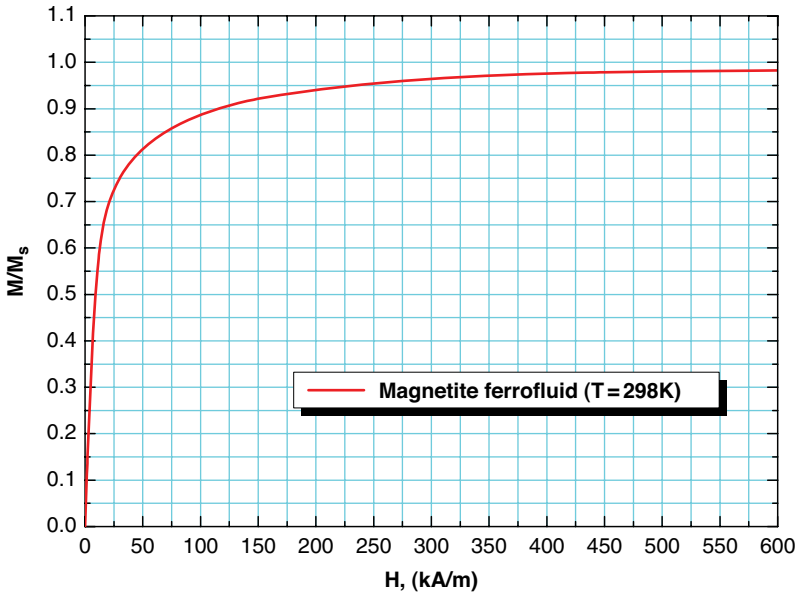

Figure 12. Variation of magnetisation with the external applied magnetic field.

4.1 The weight penalty

There is no doubt that one of the major factors to be considered in an aircraft project is the weight. In the application of the proposed method, one of the main concerns could be related to the weight of the magnets needed to attach the ferrofluid film. However, because the ferrofluid film is very thin (a few millimetres or less), it is expected that the extra weight from the train of magnets attached in the wing of the aircraft will not result in additional concerns. To assess the extra weight per surface area of the wing caused by the magnets, we proceed as follows: First, we determine the external magnetic field needed to attain the magnetic saturation of the ferrofluid. The measured magnetisation of the ferrofluid as a function of the external magnetic field is shown in Fig. 12. It is clear from this figure that, with an external magnetic field of around 100kA/m, we attain 10% of saturation (≈32kA/m), which translates into ≈3.2kA/m, which for a film of a few millimetres will result in gradients $> 10^5 \mathrm{A/m^2}$, being sufficient to guarantee strong film attachment at the wall (Fig. 3).

Second, we need to assess the amount of magnets needed to generate this magnetic field at a certain distance from the wing. To obtain an estimate of this, let us assume a wing with a certain thickness and covered by a film of ferrofluid in which there are a train of magnets attached below. The minimum skin thickness of a wing depends on several factors, for example, the load distribution, etc., and we can find commercial aircraft types, such as the 727, with a minimum skin thickness as low as 0.1mm or as high as 1.27mm for DC-8 and DC-9 aircraft. Therefore, to be on the safe and most conservative side, let us assume a thickness of around 1.27mm. On the other hand, let us consider a ferrofluid with a thickness of, say, 2mm. Therefore, the magnets will be at a distance of around 1.27mm + 2mm = 3.27mm. Then, we want to measure the magnetic field from a flat arrangement of magnets with a certain total thickness l at a distance of 3.27mm away from the surface. Finally, if it is desired to cover a surface area of the wing S_w with a ferrofluid film, then the volume of magnet V_m needed will

https://doi.org/10.1017/aer.2020.65 Published online by Cambridge University Press

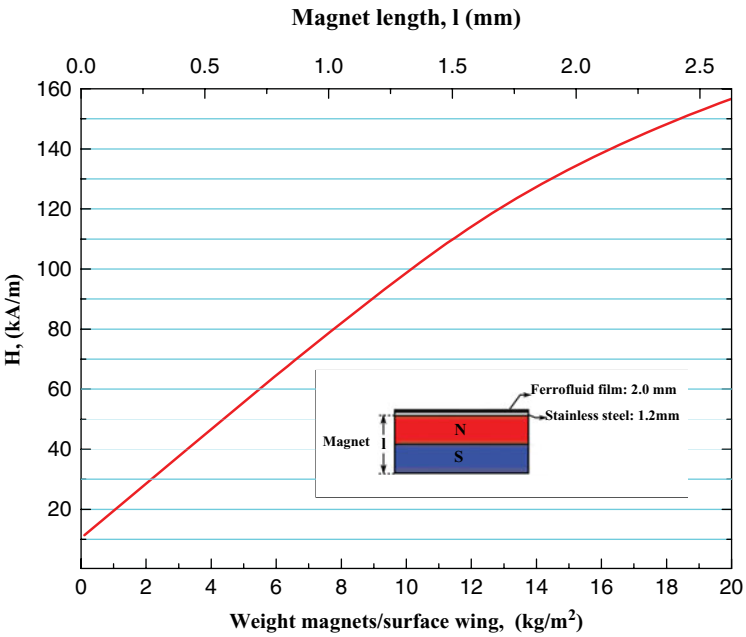

Figure 13. Magnetic field generated by a flat magnet at a distance of 3.2mm from the surface and as a function of the thickness of the magnet (upper abscissa), and the weight of the magnet per unit surface area of the wing (bottom abscissa).

be $V_m = S_w l$, and if the magnet has a density of ρ_m, this will result in a weight of $W_m = \rho_m S_w l$, with a weight of magnet per unit surface area of the wing of $\frac{W_m}{S_w} = \rho_m l$. The magnetic field as a function of the thickness of neodymium magnets, $\rho_m = 7,612 \text{kg/m}^3$, was measured, and the resulting curve is shown in Fig. 13. It is seem that, to generate the magnetic field of around 32kA/m, a density of around $\frac{W_m}{S_w} = 2.5 \text{kg/m}^2$ is required. The penalty caused by the excess weight is small compared with the lift enhancement, and will become negligible as the total weight of the aircraft increases. To see this, consider, for example, a DC-8 aircraft with a typical weight of around 130,000kg. With a lift enhancement of around 1.5, this will translate into an additional force of around 65,000kgf. However, with a wingspan of around 44m and a width of around 1m, the total surface area of the wing will be around 100m^2, which with the aforementioned calculated figure of $\frac{W_m}{S_w} = 2.5 \text{kg/m}^2$ will result in an extra weight of 2,500kg, i.e. less than 0.5%. Even assuming the most pessimistic figure, the lift gain will be much greater. It must also be noted that the above rough calculations assume covering the entire wings with a ferrofluid layer, which of course will not be the case. In fact, the ferrofluid film concept will be applied in specific regions, for example at the point where the detachment of the boundary layer occurs, in order to delay it.

ACKNOWLEDGEMENTS

This research was supported by the Spanish Ministry of Economy and Competitiveness under Ramon y Cajal fellowship grant RYC-2013-13459.

https://doi.org/10.1017/aer.2020.65 Published online by Cambridge University Press

DECLARATION OF INTERESTS

The authors report no conflicts of interest.

REFERENCES

1. MODI, V.J. Moving surface boundary-layer control: a review, *J. Fluid Struct.*, 1997, **11**, pp 627–663.
2. HAMMER, P., VISBAL, M., NAGUIB, A. and KOOCHESFAHANI, M. Lift on a steady 2-D symmetric airfoil in viscous uniform shear flow, *J. Fluid Mech.*, 2018, **837**, R2.
3. FERNANDEZ-FERIA, R. and ALAMINOS-QUESADA, J. Unsteady thrust, lift and moment of a two-dimensional flapping thin airfoil in the presence of leading-edge vortices: a first approximation from linear potential theory, *J. Fluid Mech.*, 2018, **851**, pp 344–373.
4. PANDA, J. and ZAMAN, K. Experimental investigation of the flow field of an oscillating airfoil and estimation of lift from wake surveys, *J. Fluid Mech.*, 1994, **265**, pp 65–95. doi: 10.1017/S0022112094000765
5. BHAT, S., ZHAO, J., SHERIDAN, J., HOURIGAN, K. and THOMPSON, M. Evolutionary shape optimisation enhances the lift coefficient of rotating wing geometries, *J. Fluid Mech.*, 2019, **868**, pp 369–384.
6. YEH, C. and TAIRA, K. Resolvent-analysis-based design of airfoil separation control, *J. Fluid Mech.*, 2019, **867**, pp 572–610.
7. GAO, W., ZHANG, W., CHENG, W. and SAMTANEY, R. Wall-modelled large-eddy simulation of turbulent flow past airfoils, *J. Fluid Mech.*, 2019, **873**, pp 174–210.
8. WANG, S., HE, G. and LIU, T. Estimating lift from wake velocity data in flapping flight, *J. Fluid Mech.*, 2019, **868**, pp 501–537.
9. RINGUETTE, M.J., MILANO, M. and GHARIB, M. Role of the tip vortex in the force generation of low-aspect-ratio normal flat plates, *J. Fluid Mech.*, 2007, **581**, pp 453–468.
10. GILARRANZ, J., TRAUB, L. and REDINIOTIS, O. A new class of synthetic jet actuators-part II: application to flow separation control, *Trans. ASME-I J. Fluid Eng.*, 2005, **127**, (2), p 377.
11. ROSENWEIG, R.E. *Ferrohydrodynamics*, Dover, 1985, Mineola, NY.
12. LANDAU, L.D. and LIFSHITZ, E.M. *Fluid Mechanics*, 2nd ed, Pergamon Press, 1989.
13. BATEMAN, H. *Partial Differential Equations of Mathematical Physics*, Cambridge University Press, 1932, Cambridge, UK, p. 175.
14. BOUKENKOUL M.A., LI, F.-C., CHEN, W.-L. and ZHANG, H.-N. Lift-generation and moving-wall flow control over a low aspect ratio airfoil. *J. Fluid Eng.*, 2018, **140**, (1), p. 011104.